TAO, Vol. 9, No. 3, 509-532, September 1998

New Gravity and Magnetic Anomaly Maps in the Taiwan-Luzon Region and Their Preliminary Interpretation

Shu-Kun Hsu[1], Char-Shine Liu[2], Chuen-Tien Shyu[2], Shao-Yung Liu[2], Jean-Claude Sibuet[3], Serge Lallemand[4], Chengsung Wang[5], and Donald Reed[6]

(Manuscript received 3 March 1998, in final form 4 Ausust 1998)

ABSTRACT

We have compiled new free-air gravity anomaly (FAA) and magnetic anomaly maps, shedding light on the tectonics in the Taiwan-Luzon region. To have a suitable datum level for both the available gravity and magnetic anomaly data, the set of data from an ACT cruise, conducted during May 27 to June 21, 1996, was chosen as a reference. Based on the cross-over error analysis, all the other data were adjusted accordingly. Some satellite-derived, airborne or land data were also added to the compilation to obtain better coverage.

Several major new insights into the Taiwan-Luzon region are revealed by the new maps. (1) A prominent NE-SW trending belt of gravity and magnetic anomalies is present in the onshore and offshore areas of southwestern Taiwan. The Peikang High is located on this belt. (2) Located in the offshore region west of Taiwan and to the north of the belt described above, the Taishi Basin, in contrast, occupies a relatively low FAA area. It could be regarded as a flexural basin on account of the loading of a thrust-and-fold belt in western Taiwan. (3) A probable NW-SE trending old transform fault is well imaged off southwestern Taiwan, which separates the lithosphere (plate) of the South China Sea from a trapped piece of the Philippine Sea plate. (4) Located east of the Luzon Arc, the Huatung Basin contains several E-W trending magnetic reversals and two N-S trending old fracture zones. The Huatung Basin is separated from the West Philippine Basin by the "123E Fracture Zone". Accordingly, the Gagua Ridge corresponds to a transverse ridge bounding the 123E Fracture Zone. (5) The Luzon Arc is abnormally concave toward the Manila Trench and becomes

[1] Institute of Geophysics, National Central University, Chungli, Taiwan, ROC
[2] Institute of Oceanography, National Taiwan University, P.O. Box 23-13, Taipei, Taiwan, ROC
[3] Ifremer, Centre de Brest, 29280 Plouzané, France
[4] UMR 5573, Laboratoire de Géophysique et Tectonique, Université de Montpellier 2, France
[5] Institute of Applied Geophysics, National Taiwan Ocean University, Keelung, Taiwan, ROC
[6] Department of Geology, San Jose State University, San Jose, CA 95192, USA

wider toward the south. The internal deformation of the Luzon Arc in terms of several NE-SW discontinuities could be related to its collision with eastern Taiwan. (6) Three previously proposed NW-SE trending strike-slip faults in the southern Okinawa Trough, west of 123.5° E, are well imaged on both the FAA and magnetic anomaly maps. Post-collisional volcanism off northeastern Taiwan occurs along these NW-SE trending faults.

(Key words: Free-air gravity anomaly, Bouguer anomaly, Magnetic anomaly, Transverse ridge, Fracture zone, Transform fault, Taiwan)

1. INTRODUCTION

Gravity and magnetic anomaly maps generally provide fundamental reconnaissance of a geological province. These maps yield basic information reflecting the physical properties of the underlying rocks or sediments.

Since the advent of satellite altimetry, a better coverage and resolution of sea surface reliefs can be obtained. As a result, global satellite-based marine gravity anomaly maps have been deduced on the basis of the calculated geoid heights (e.g. Hwang and Parsons, 1996; Sandwell and Smith, 1997). These data can be useful for exploring areas where there is no or few marine data. However, the accuracy and resolution of the gravity field recovered from satellite altimetry is limited due to the short-wavelength noise from ocean surface waves (typically > 1 m), especially from ocean tides on the continental shelves (Sandwell and Smith, 1997).

A fairly complete gravity survey on Taiwan was done by Yen *et al.* (1990). Their free-air gravity anomaly (FAA) map updated several previous studies (e.g. Chang and Hu, 1981; Hu and Chen, 1986). The FAA map from Yen *et al.* (1990) was later included with available shipboard gravity data (e.g. Liu *et al.*, 1992) to produce a regional FAA map of onshore and offshore Taiwan (Yen *et al.*, 1995). Since then, through bilateral cooperation in marine geology and geophysics between Taiwan and Russia, Taiwan and France, and Taiwan and the U.S.A., a significant amount of marine geophysical data around Taiwan have been collected. As a benchmark, the two most complete cruises covering most of the offshore area around Taiwan are the EW9509 cruise in 1995 and the ACT cruise in 1996 (Figure 1). With these significant additional data, we have compiled a new regional FAA map with a view to better understanding the tectonic problems in the Taiwan region.

On the other hand, no systematic magnetic survey has been conducted for Taiwan island. This is probably due to the difficulty of the field work. However, a few magnetic data were collected on the periphery of Taiwan: the Coastal Plain in western Taiwan (Chang and Hu, 1981), the Pingtung Plain in southwestern Taiwan (Yu and Tsai, 1981), the Coastal Range of eastern Taiwan (Hu and Chen, 1986; Wu, 1991), the Ilan Plain of northeastern Taiwan (Yu and Tsai, 1979; Hsu *et al.*, 1996a), and the Tatun volcanic region of northern Taiwan (Yang *et al.*, 1994).

In 1968, an aeromagnetic survey of offshore western Taiwan was flown at 150 m above

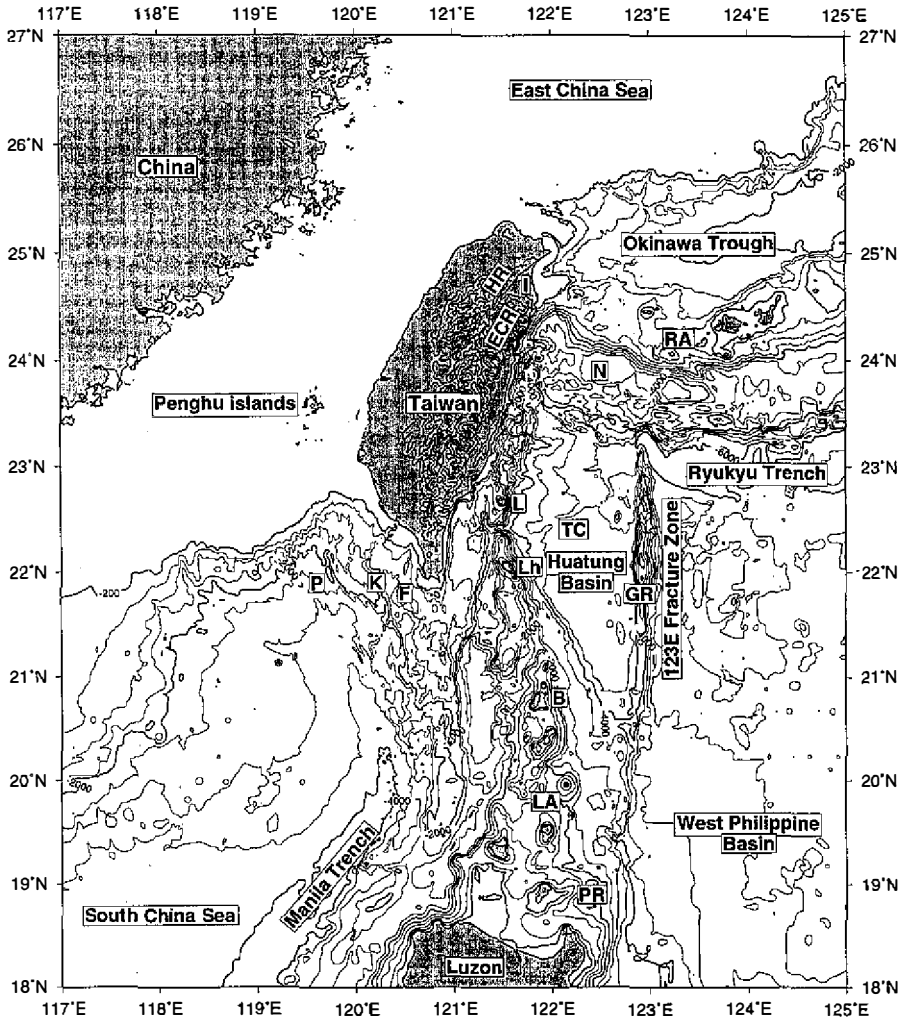

Fig. 1. The bathymetric map in the Taiwan-Luzon region. B = Batan islet; ECR = eastern Central Range; F = Fangliao Canyon; GR = Gagua Ridge; HR = Hsüehshan Range; I = Ilan Plain; K = Kaoping Canyon; L = Lutao islet; LA = Luzon Arc; Lh = Lanhsu islet; N = Nanao Basin; P = Penghu Canyon; PR = Palaui Ridge; RA = Ryukyu Arc; TC = Taitung Canyon;

sea level by the U.S. Naval Oceanographic Office as part of the Magnet Project (Bosum *et al.*, 1970; Hu and Lu, 1979). It still plays an important role in understanding the magnetic features off western Taiwan. For other offshore areas, other than the data acquired from two French cruises (POP1 and POP2 in 1984; Sibuet *et al.*, 1987), during the 1970s and 1980s magnetic data were principally collected by the Institute of Oceanography of National Taiwan University (e.g. Lee and Hilde, 1971; Wang and Hilde, 1973; Shyu and Chiao, 1983; Hilde and Lee,

1984; Shyu and Chen, 1991), and under Taiwan-US cooperation (Bowin *et al.*, 1978). The quality of marine magnetic data was improved after the employment of the Global Positioning System in the 90's (e.g. Yu and Shyu, 1994; Shyu *et al.*, 1996).

A magnetic anomaly map is certainly important to investigations of regional tectonics by providing information in geological boundaries and the volcanic nature of underlying sources. Therefore, we attempt to compile all the existing magnetic data. However, the available cruise tracks are too sparse to produce a regional, evenly distributed magnetic anomaly map (cf. Oshida *et al.*, 1992). Finally, we present a general description of tectonics around Taiwan in the light of these newly compiled potential maps.

2. DATA REDUCTION AND COMPILATION

During May 27 to June 21, 1996, the ACT marine geophysical cruise was conducted in the context of Sino-French oceanographic cooperation with the purpose of understanding the offshore portions of the Taiwan subduction/collision complex (Lallemand *et al.*, 1997). Because tracks of this cruise cover a large area offshore from eastern and southwestern Taiwan, the ACT cruise becomes a suitable reference for the adjustment of other marine gravity and magnetic data. The total length of the ACT cruise tracks, including a preceding two-day transit, is about 10,360 kilometers. The analysis of intersection errors (cross-over errors) will be used to indicate data quality and adjust the datum level of each cruise (Hsu, 1995). Though the spatial resolution of each map is different (see later), we have produced each map with a constant grid spacing of one arc-minute.

2.1 Gravity data

2.1.1 ACT and EW9509

For the ACT cruise, the *R/V l'Atalante* KSS30 gravimeter was tied on IGSN 71 system at quay E2 (standard value of 978974.04 mGal) before leaving Keelung. At the end of the ACT cruise, the gravimeter was tied again at quay 17 in Kaoshiung (978780.57 mGal). During the cruise, a major instrumental drift of 500 mGal occurred at around 21:00 on June 17. Then a nonlinear drift of ~44 mGal persisted for about two hours and thirty minutes. A second drift of ~44 mGal occurred from 12:08 to 12:17 on June 18. The gravity anomaly data during the periods of nonlinear drift could not be recovered. However, before 21:00 on June 17, the mean error of the overall cross-over errors of the ACT cruise is only 0.3 mGal and a standard deviation of only 2.6 mGal (Figure 2). The useful ACT gravity data after 21:00 on June 17 could be recovered by comparing the ACT data with the EW9509 data. As a matter of fact, prior to the major instrumental drift, the analysis of the external cross-over errors between these two cruises indicates that the gravity data of both cruises are quite consistent, except that the datum level of the EW9509 cruise is 1.1 mGal higher than the ACT cruise (Figure 2). After adjusting the EW9509 datum level to that of the ACT datum level, most of the ACT data after 21:00 on June 17 were restored by cross-over error analysis.

2.1.2 Other data

Other cruises providing gravity data are listed in Table 1. Most of these data near Taiwan

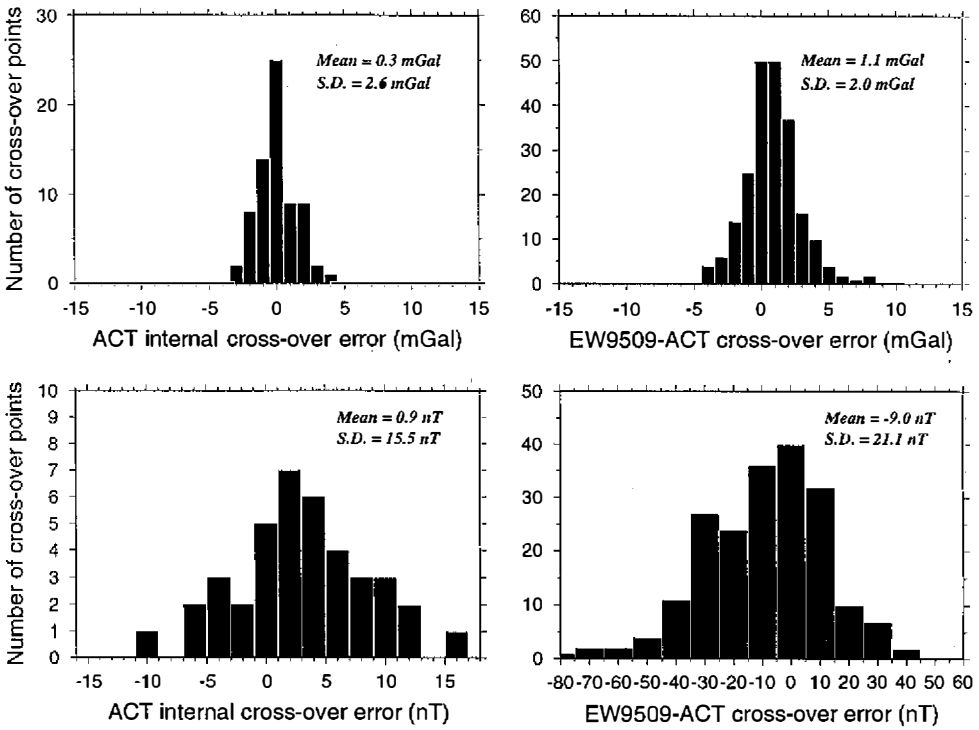

Fig. 2. (left up) Internal cross-over errors of the ACT FAA. (left down) Internal cross-over errors of the ACT magnetic anomalies. (right up) Cross-over errors of the FAA between the EW9509 and ACT cruises. (right down) Cross-over errors of the magnetic anomalies between the EW9509 and ACT cruises. S.D. = standard deviation.

were provided by the MW9006, PG13, PG15, POP1 and POP2 cruises. GPS navigation was used during these five cruises and the quality of data is good (e.g, Liu, 1993). Their mean error and standard deviation relative to the ACT cruise are: -0.1 and 3.3 mGal, 1.0 and 8.4 mGal, -0.6 and 2.9 mGal, -0.6 and 4.6 mGal, and 0.6 and 3.9 mGal, respectively. Other shipboard gravity data came from the National Geophysical Data Center data set of the National Oceanic and Atmospheric Administration (NOAA), USA. However, because of positioning problems, cruise data using Transit navigation provide lower quality data. The datum level for each cruise was adjusted with respect to the ACT cruise. The mean error of the total shipboard gravity data in positive difference statistics (Swan and Young, 1978) is 6.3 mGal, and the standard deviation is 11.2 mGal (Figure 3). The spatial distribution of the observed points is shown in Figure 4. It is noted that the points acquired during the ship gyrations were removed to avoid large errors.

In order to provide a more comprehensive view of the gravity field around Taiwan, we compiled the Taiwan FAA by Yen *et al.* (1990) with the shipboard data. Moreover, even

Table 1. Cruise names and years (in parentheses) of shipboard gravity data used in the compilation.

ACT(1996)	C1217(1969)	C1404(1971)	C1710(1974)	C1711(1974)
C2006(1976)	C2007(1976)	C2008(1976)	C2009(1977)	C2612(1985)
C2614(1985)	DME10(1973)	DME24(1980)	ESTASE2(1984)	EW9509(1995)
GH7501(1975)	HS7602(1976)	HS7603(1976)	HS7905(1979)	HS8003(1980)
HS8202(1982)	HT8402 (1984)	HT8403 (1984)	HT8502(1985)	INDP03WT(1976)
INDP05WT(1976)	KH7104 (1971)	KH7201(1972)	KH7403(1974)	KH7605(1976)
KH79(1979)	MW9006(1990)	PG13(1994)	PG15(1994)	POL7201(1972)
POP1(1984)	POP2(1984)	RN86(1986)	RN87(1987)	RN88(1988)
SINKO(1984)	V2110(1965)	V2405(1967)	V2406(1967)	V2817(1971)
V3309(1976)	V3310(1976)	V3404(1977)	V3604(1979)	V3608(1980)
V3609(1980)	V3613(1980)	V3614(1980)		

though the satellite-derived marine gravity anomalies have a limit of short wavelength (Small and Sandwell, 1992; Sandwell and Smith, 1997), we used them to fill in areas of large data gaps in our compiled region (Figure 4). Satellite data in the nearshore areas of Taiwan were not used in order to avoid large errors due to ocean tides. Finally, an FAA map around Taiwan was generated using the GMT software package (Wessel and Smith, 1991; Figure 5).

2.1.3 Bouguer anomaly map

It is well-known that the FAA is dominated by the topographic effect. To mitigate the topographic effect, Bouguer and terrain corrections were applied to the data. This was done by removing the gravity effect caused by the terrain above sea level and replacing the sea water with sediments. As a first order approximation, the densities of land terrain and marine sediments were assumed to be 2.6 and 1.8 g/cm^3, respectively. The resulting Bouguer anomaly map around Taiwan is shown in Figure 6.

2.2 Magnetic Data

2.2.1 ACT and EW9509

The geomagnetic data acquired during the ACT and EW9509 cruises were reduced to magnetic anomalies by subtracting the total field given by the IGRF1995 model (IAGA, 1996). The diurnal variation near Taiwan can reach tens of nanoteslas(nT) (Regan and Rodriguez, 1981), consequently it was removed from the magnetic anomalies by taking into account the geomagnetic variations recorded at several permanent observatories on Taiwan. The analysis of internal cross-over errors for the ACT magnetic anomaly data gives a mean error and the standard deviation of 0.9 nT and 15.5 nT, respectively. This result shows better quality than cruise MW9006 (-6.0 nT and 25.5 nT, respectively).

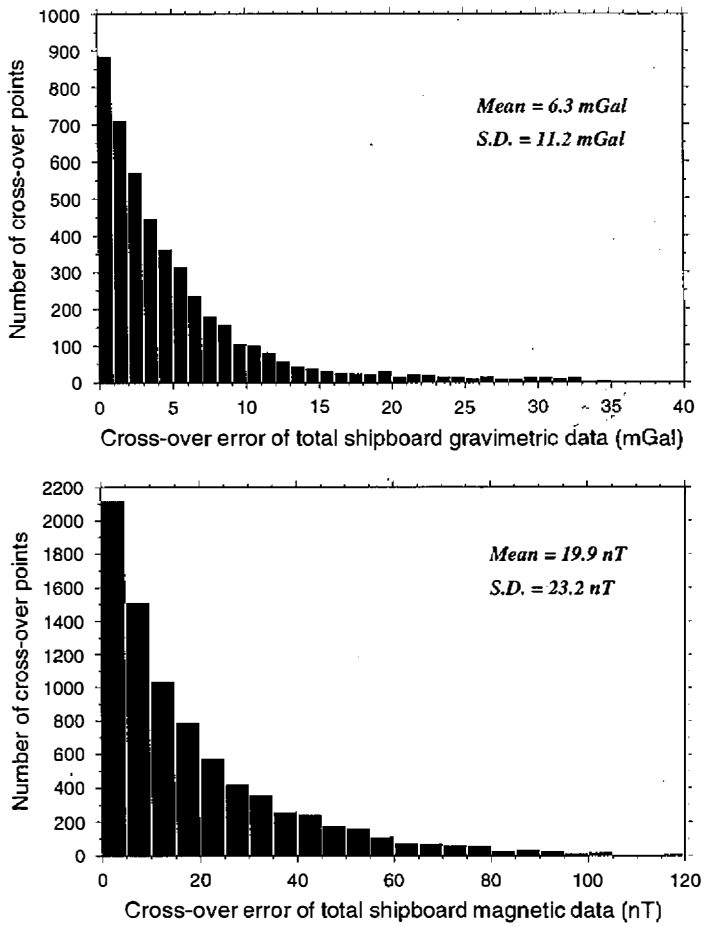

Fig. 3. (up) Cross-over errors of total shipboard FAA data in positive difference statistics. (down) Cross-over errors of total shipboard magnetic anomalies in positive difference statistics. S.D. = standard deviation.

A comparison of EW9509 and ACT magnetic data shows that EW9509 also has good data quality except for a -9 nT offset of the datum level (Figure 2). After adjusting the datum level, the EW9509 data also provide a good reference frame for correcting magnetic data from other cruises which do not intersect ACT tracks.

2.2.2 Other data

Other magnetic data used in Figure 8 include shipboard data off Taiwan (Figure 7), aeromagnetic data off western Taiwan (Bosum *et al.*, 1970) and some land observations along the periphery of Taiwan (Chang and Hu, 1981; Yu and Tsai, 1981; Hsu *et al.*, 1996a). The magnetic data in the Coastal Range of eastern Taiwan were not included in the compilation because of their positioning uncertainty (Yu-Ming Wu, personal communication). The reduction

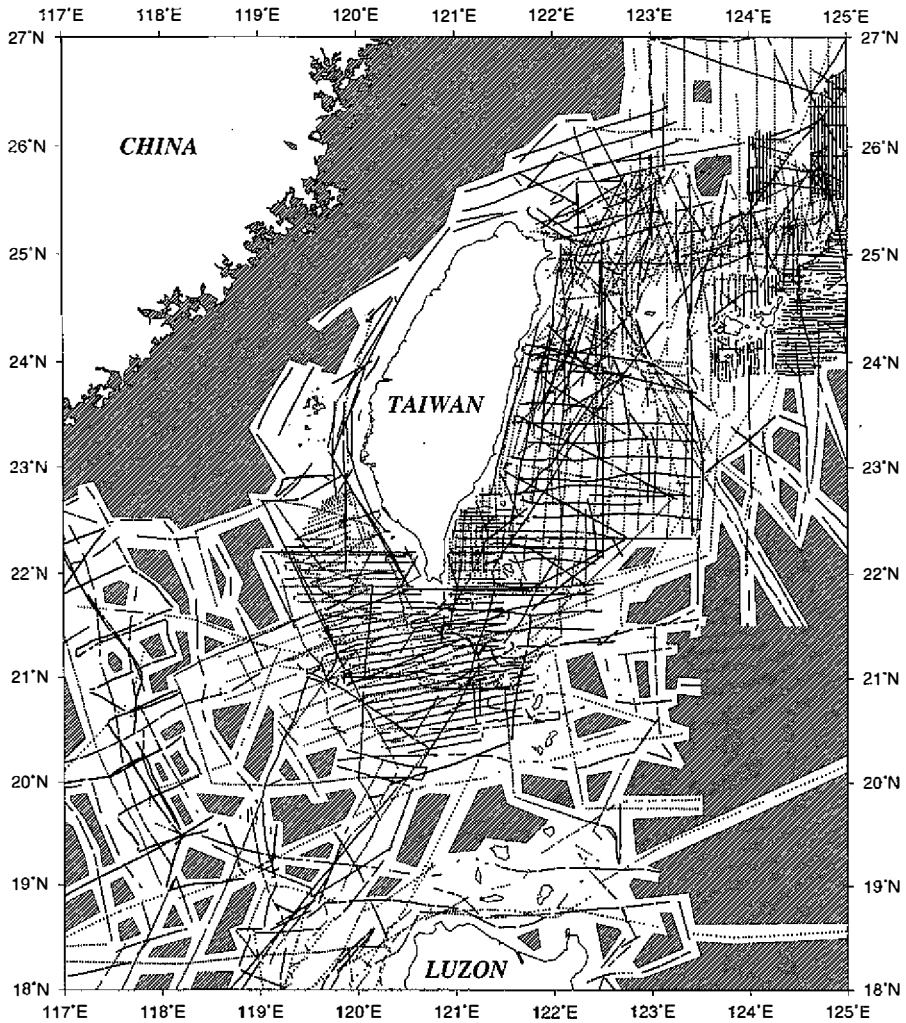

Fig. 4. Distribution of shipboard gravity data used in the compilation (represented by dotted points). Shaded areas represent satellite-derived marine data used in the compilation.

of all available data was based on the IGRF1995 model (IAGA, 1996) and the ACT datum level was used as a reference to adjust all the other datasets. The cruises providing magnetic data are listed in Table 2. Besides ACT and EW9509, significant data for map compilation were provided by MW9006, PG13, PG15, POP1 and POP2 cruises. Their mean errors and standard deviations relative to the ACT cruise are -41.9 and 18.9 nT, -4.1 and 6.9 nT, -4.2 and 7.6 nT, 4.5 and 18.6 nT, and -24.0 and 29.5 nT, respectively. Except for different datum levels, they are of good quality. Before the adjustment of datum level, the mean error and standard deviation (in positive difference statistics) of all the shipboard magnetic data in this compila-

Table 2. Curise names and years (in parentheses) of shipboard magnetic data used in the compilation.

ACT(1996)	ANTP04MV(1970)	C1217(1969)	C1404(1971)	C1710(1974)
C1711(1974)	C2006(1976)	C2007(1976)	C2008(1976)	C2009(1977)
C2612(1985)	C2614(1985)	DELP88K5(1988)	DSDP31GC(1973)	EW9509(1995)
GH7501(1975)	HS7905(1979)	HS8003(1980)	HT8402 (1984)	HT8403 (1984)
INDP03WT(1976)	KH7104 (1971)	MW9006(1990)	ODP124EJ(1989)	ORI279(1991)
ORI298(1991)	ORI320(1992)	ORI325(1992)	ORI326(1992)	ORI336(1992)
ORI355(1993)	ORI363(1993)	ORI367(1993)	ORI379(1994)	ORI392(1994)
ORI395(1994)	ORI423(1995)	ORI486(1997)	ORI492(1997)	ORI495(1997)
PG13(1994)	PG15(1994)	POL7201(1972)	POP1(1984)	POP2(1984)
RN86(1986)	RN87(1987)	RN88(1988)	SINKO(1984)	V2110(1965)
V2405(1967)	V2406(1967)	V2817(1971)	V3309(1976)	V3310(1976)
V3404(1977)	V3604(1979)	V3608(1980)	V3609(1980)	V3613(1980)
V3614(1980)				

tion is 38.4 and 80.9 nT, respectively. After adjustment, these are reduced to 19.9 and 23.2 nT, respectively (Figure 3). In order to have a more complete coverage, the aeromagnetic data in southeastern China from Magnetic Anomaly Map of East Asia (1994) were also included in Figure 8.

3. MAJOR CHARACTERISTICS OF GRAVITY AND MAGNETIC ANOMALIES

Several important features can be identified on the compiled gravity and magnetic anomaly maps (Figures 5 and 8).

3.1 NE-SW Trending Features Off Western Taiwan

Magnetic and gravity anomalies of the western Taiwan continental shelf show NE-SW trends which reflect the rifted Chinese continental margin (Yu, 1994) or the relict arcs and backarc basins (Sibuet and Hsu, 1997). The high-positive amplitude and linear magnetic anomaly trending NE-SW both onshore and offshore from southwest Taiwan is very prominent. This linear belt is generally associated with a negative magnetic anomaly belt to its north, showing a dipole magnetic field. The Peikang High in southwestern Taiwan is located on this belt. Due to lack of magnetic data in the northern and eastern half of Taiwan, the northward continuation of this belt is not clear. However, the Taiwan-Sinzi Folded Zone, showing a similar amplitude character, may be related to this belt (Lee and Lu, 1976; Hsu and Sibuet, 1995). In western Taiwan, the area around 120.8° E and 24.4° N exhibits relatively low gravity anomalies (Figure 5) and corresponds to the location of the Taishi Basin (see Chi, 1996; Sibuet and Hsu, 1997). Because the Taishi Basin is located immediately west of the Taiwan orogenic belt, it could be interpreted as a flexural basin caused by loading from the

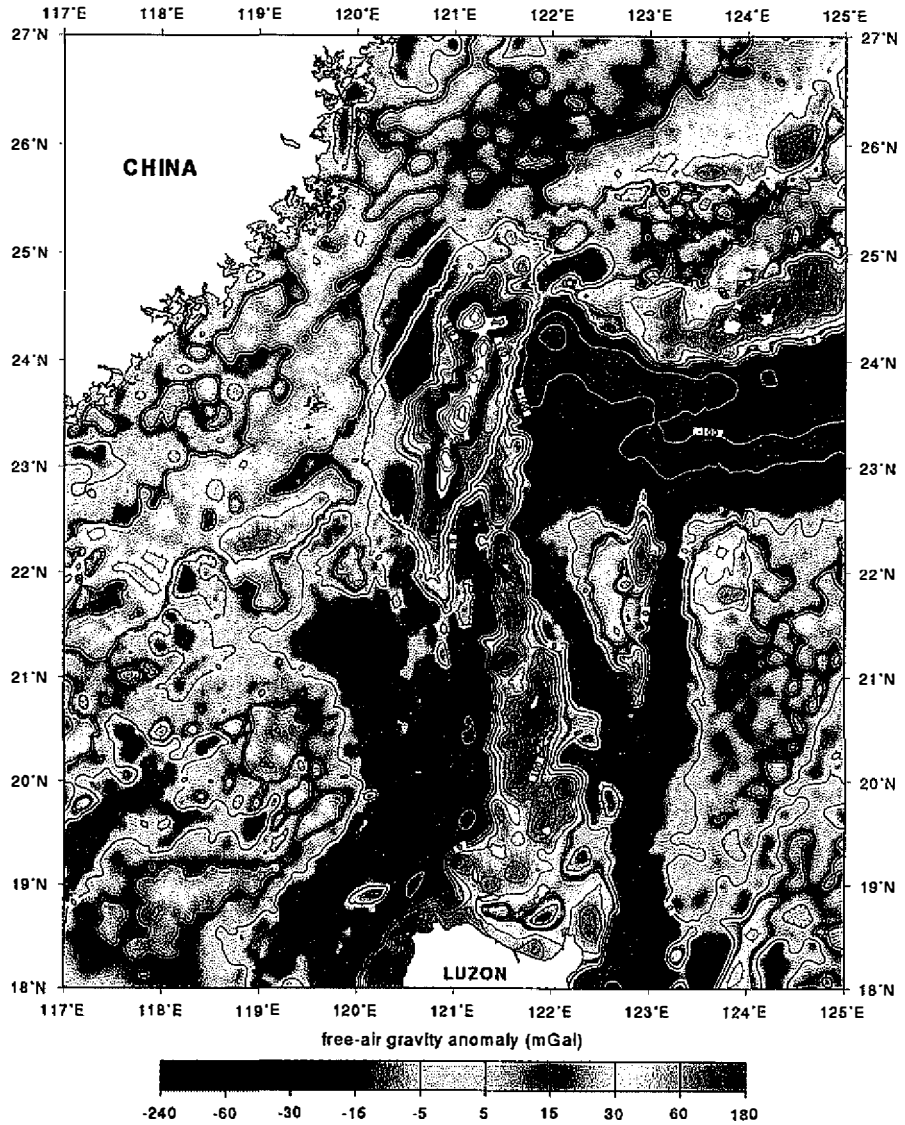

Fig. 5. Free-air gravity anomaly map in the Taiwan-Luzon region. The land data of Yen *et al.* (1990) was incorporated. Contour interval is 20 mGal.

west-vergent thrusts and folds. The loading of sequential thrust units is demonstrated by low heat flow values in western Taiwan (Lee and Cheng, 1986; Hwang and Wang, 1993). Note that, besides the Taishi Basin, the onshore/offshore area along western Taiwan is associated with low Bouguer anomalies (Figure 6), which confirms that western Taiwan is more or less subjected to flexural bending in response to the load of the west-vergent thrust-and-fold belt.

Off southwestern Taiwan, a large amount of sediment has been deposited since 5 Ma in

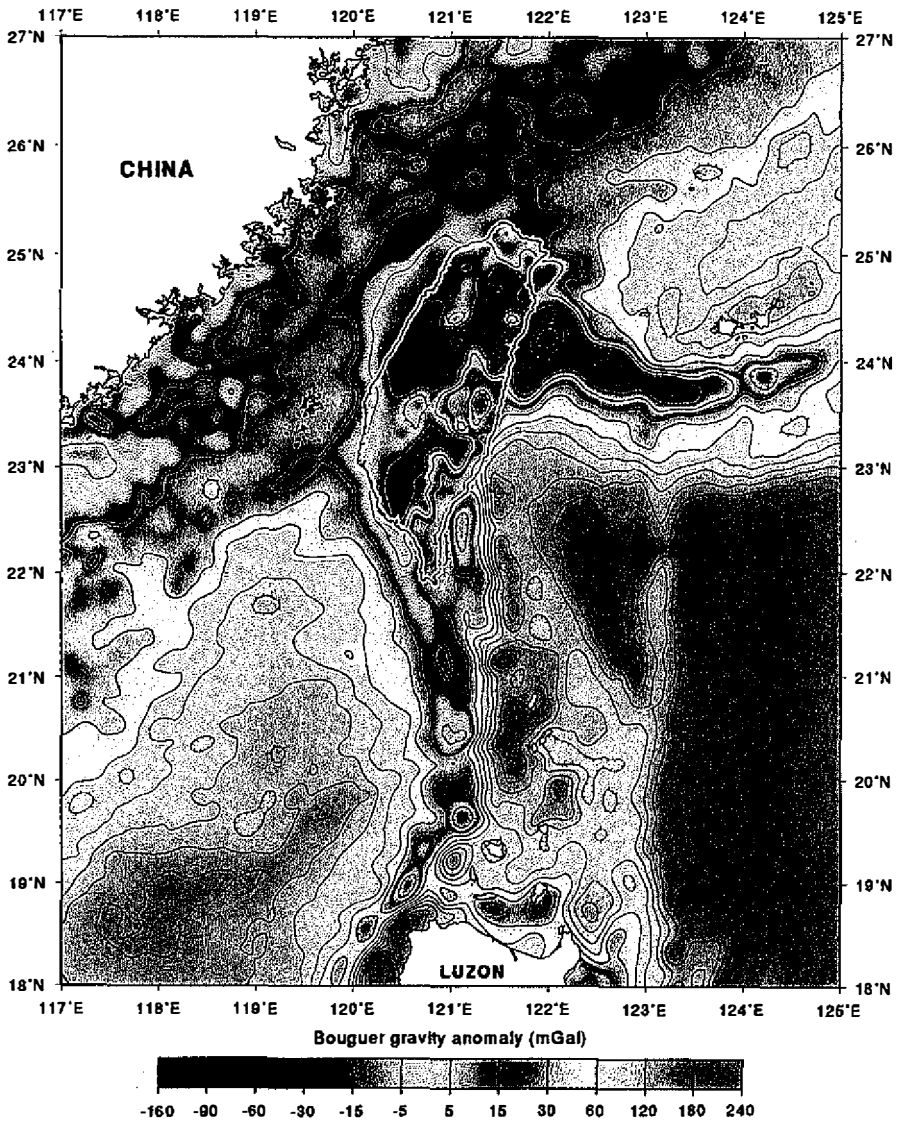

Fig. 6. Bouguer anomaly map in the Taiwan-Luzon region. Contour interval is 20 mGal.

response to the uplift and erosion of the Taiwan mountain belt (e.g. Lee, 1993). Due to the convergence between the Philippine Sea Plate and the Eurasian Plate, the sediments have been deformed in terms of thrusts or strike-slip faults. The Penghu Canyon (Yu and Lee, 1993), located along the southeastern slope of the relict Tainan Arc (Sibuet and Hsu, 1997), is well-marked by a linear low FAA trending NE-SW (Figures 1 and 5). The thrust front off southwestern Taiwan directly abuts the Penghu Canyon. It is noted that the thrust front described by

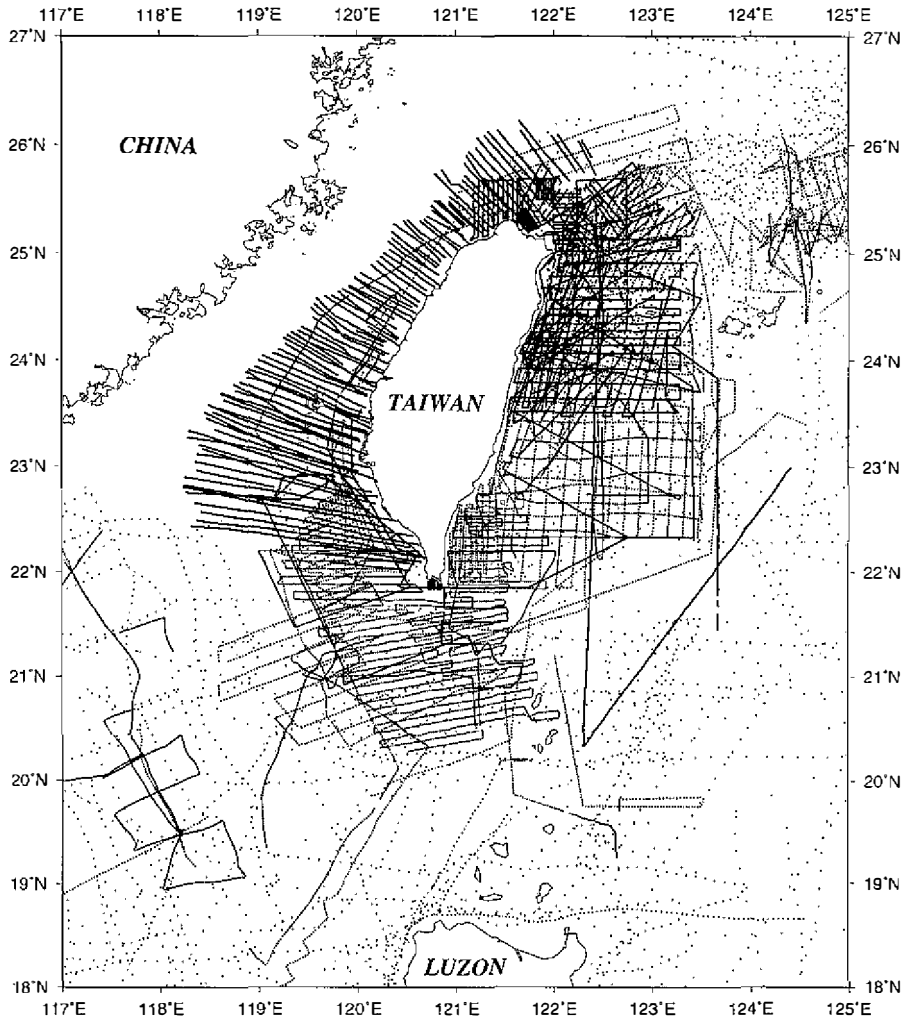

Fig. 7. Distribution of shipboard magnetic data (represented by dotted points). Aeromagnetic data off western Taiwan were downward continued to sea level.

Lee (1993) and recently redrawn in detail by Liu *et al.* (1997a) is located within this low FAA stripe. The intensive thrusts distributed between the Penghu Canyon and the Kaoping Canyon (Reed *et al.*, 1992; Liu *et al.*, 1997a) are associated with a relatively high FAA. Further east, a linear low FAA is linked to the location of the Fangliao Canyon (Yu and Lu, 1995), the possible offshore continuation of the N-S trending Chaochou Fault on Taiwan. Off southern Taiwan, the magnetic anomalies display ENE-WSW trends, instead of the general NNW-SSE trend of thrusts. This implies that the thrust deformation off southern Taiwan involves only the upper sediments but not the underlying basement.

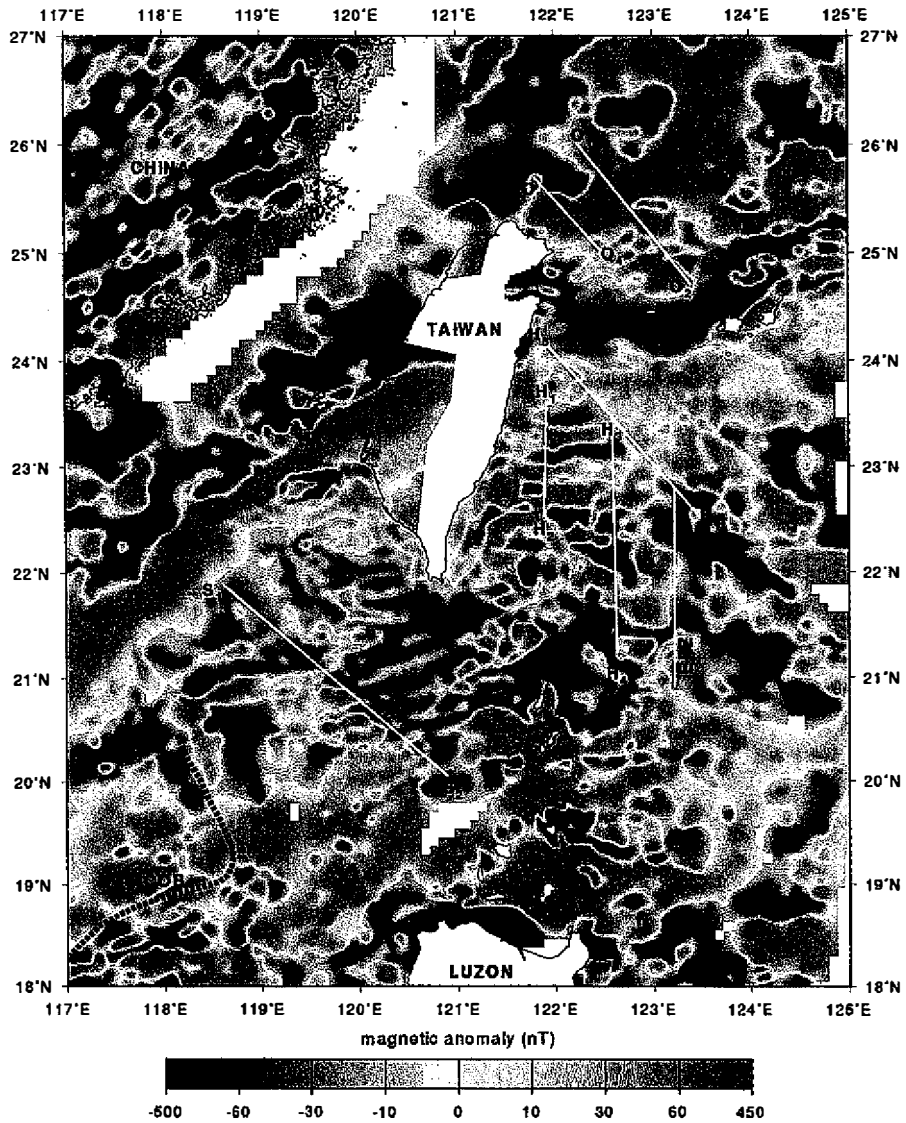

Fig. 8. Magnetic anomaly map in the Taiwan-Luzon region. COB = continent-ocean boundary.

3.2 An old transform fault between the South China Sea plate and a trapped piece of the Philippine Sea Plate

On each side of segment S_1S_2 in Figure 8, the pattern of magnetic anomalies displays different signatures: low-amplitude signatures to the northeast and high-amplitude signatures to the southwest. The existence of this boundary is also suggested in the FAA map (figure 5):

low FAA to the northeast and high FAA to the southwest of this boundary. In the Bouguer anomaly map (Figure 6), this boundary corresponds to a location of relatively high gradients of gravity anomalies. Additionally, a seamount is located on the boundary (Figure 2a of Hsu *et al.*, 1996b). The gravity and magnetic anomalies seem to suggest that the oceanic basement is deeper on the northeastern side; hence, the basement on the northeast side of S_1S_2 should be older than on the southwest side. The contrast in basement depth along S_1S_2 has been confirmed by seismic reflection profiles (Sibuet *et al.*, in preparation). Near point S_1, the structural trends, as revealed by the FAA, roughly change their orientations from NE-SW on the northeast side, to NW-SE on the southwest side. Therefore, the S_1S_2 boundary may represent an old transform fault, separating the lithosphere of the South China Sea from a trapped piece of the Philippine Sea Plate (Hsu and Sibuet, 1995; Sibuet and Hsu, 1997); however, its position, as revealed by these newly compiled gravity and magnetic anomaly maps, is slightly different from that previously proposed by Hsu and Sibuet (1995) and Sibuet and Hsu (1997).

The E-W to ENE-WSW trending magnetic lineations southwest of the boundary S_1S_2 are likely to be magnetic reversals of the ocean floor. To date, the greatest age in the South China Sea has been identified as *Anomaly 11* (ca. 30 Ma) which trends NE-SW near 118.2° E and 19° N, close to the suggested continent-ocean boundary (COB, white dashed line in Figure 8) (Taylor and Hayes, 1983; Briais *et al.*, 1993; Cande and Kent, 1995). The suggested position of the COB can be roughly traced along the zero-contour line in the FAA map (Figure 5). It is interesting to note that the magnetic reversals we suggested are located further northeast than *Anomaly 11*. That is, they are present to the north of the previously proposed COB. Because the existing magnetic isochrons in the South China Sea (*Anomaly 5c - Anomaly 11*) indicates that the South China Sea developed from northeast to southwest (Briais *et al.*, 1993), the initial opening of the South China Sea could be elder than currently believed.

3.3 The "123E Fracture Zone" and the Gagua Ridge

From the FAA map (Figure 5), a N-S trending linear gravity low (as low as -70 mGal) located to the east of the Gagua Ridge is clearly observed. This feature is also clearly marked in the Bouguer anomaly map (Figure 6). For the sake of description, this N-S trending deep depression, directly abutting against the Gagua Ridge on the west, is named the "123E Fracture Zone (EFZ)" (Figure 1). The name is chosen to indicate its location along 123.2°E longitude. The lack of a symmetric FAA signature across the Gagua Ridge is not consistent with a linear volcanic extrusion on oceanic crust. The oceanic crust west of the EFZ belongs to the Huatung Basin and east of the EFZ to the West Philippine Basin. Because the magnetic anomalies show different orientations on each side of the EFZ (Hilde and Lee,1984), it demonstrates the necessity of introducing the EFZ, instead of the Gagua Ridge, to distinguish the two basins. The Gagua Ridge, bordering the EFZ and composed of bathymetric ridges (or seamounts) and valleys, is an uplifted sliver of oceanic crust (e.g. Mrozowski *et al.*, 1982; Hilde and Lee, 1984; Deschamps, 1997; Karp *et al.*, 1997). The magnetic anomalies of the Gagua Ridge and the Huatung Basin seem to display similar signatures (Figure 8), which suggests that the Gagua Ridge could be similar in nature to the Huatung Basin. Accordingly, the Gagua Ridge is a transverse ridge (with respect to the trend of a spreading ridge) bordering the EFZ. In fact, in

addition to the Gagua Ridge, there are several small N-S trending morphological ridges which are located directly west of the Gagua Ridge and one east of the EFZ (Hsu *et al.*, 1996b). Some of the ridges, revealed by seismic reflection profiles, are completely buried by sediments (e.g. Mrozowski *et al.*, 1982; Lewis and Hayes, 1989; Chen *et al.*, 1996; Deschamps, 1997). These ridges or seamounts to the west of the EFZ generally deepens westward. Their presence indicates that compressive deformation occurred along the EFZ, resulting in a stripe of uplifted ridges or seamounts; among these, the Gagua Ridge is the largest one. However, because strike-slip faults seem to present along the axis of the Gagua Ridge, Deschamps *et al.* (1997) proposed that the axis of the Gagua Ridge corresponds to the closure of a fracture zone. During the transpressive period, the Gagua Ridge was formed as a result of reverse faulting.

Several mechanisms can produce transverse ridges (e.g. Sandwell, 1984; Abrams *et al.*, 1988). Because the magnetic anomalies on both sides of the EFZ display different trends (Figure 8), the origin of the EFZ up-faulted ridges or seamounts must be associated with oblique compression and vertical tectonism due to changes of plate motion (e.g. Bonatti,1978; McCarthy *et al.*, 1996). Oblique compression may induce strike-slip faulting along the Gagua Ridge as observed by Deschamps *et al.* (1997). However, when did the EFZ and EFZ transverse ridges form? To answer this question, we should first note that seismic reflection profiles across the Gagua Ridge and the EFZ show no evidence of recent compressive deformation of the near-surface sediments overlying the EFZ (Lewis and Hayes, 1989).The EFZ hence represents a remnant feature. Earthquakes and basement faulting are, however, present in the Huatung Basin (Yeh *et al.*, 1991; Lewis and Hayes, 1989; Hsu *et al.*, 1996b). For example, the most significant topographic feature is the NE-SW trending Taitung Canyon, which bisects the Huatung Basin and may have partly developed along a right-lateral strike-slip fault (Hsu *et al.*, 1996b; Sibuet and Hsu, 1997). Deformation of the Huatung Basin may be related to its subduction beneath the south Ryukyu Arc and collision on the west with the island of Taiwan.

The West Philippine Basin is composed of two distinctly different spreading phases: a first phase from *Anomaly 26* to *Anomaly 20* (~58 - 43 Ma), spreading in a NE-SW direction at a rate of ~44 mm/yr; and a second phase from *Anomaly 19* to *Anomaly 13* (~41 - 33 Ma), spreading in a N-S direction at a rate of ~18 mm/yr (Hilde and Lee,1984; Cande and Kent, 1995). Because the spreading direction of the Huatung Basin is NS and the EFZ is NS trending, the development of the Huatung Basin could be related to the second phase of the West Philippine Basin. In that case, the EFZ and the associated EFZ transverse ridges could have developed during or just after the period between 41 and 33 Ma ago. It raises, however, an important issue: how is the Huatung Basin related to the second phase of spreading in the West Philippine Basin? Hilde and Lee (1984) proposed that the magnetic anomalies close to the Ryukyu Trench (between ~124° E and ~126° E) belong to the second phase; nevertheless, the swath bathymetric data to the east of the EFZ indicates that the rifting fabrics is in favor of first phase (Hsu *et al.*, 1996b). In other words, the Huatung Basin might be completely isolated from the second phase of the West Philippine Basin. Therefore, if the Huatung Basin is related to the second phase of spreading in the West Philippine Basin, then there must have been a major northward jump of the spreading ridge at the western end of the second phase West Philippine Basin, which connected eastern end of the spreading ridge of the Huatung Basin by a major transform fault. Otherwise, a "synchronous" development of the Huatung Basin and

the second phase of the West Philippine Basin had to happen, suggesting a major plate reorganization in favor of the spreading in a N-S direction (relative to the present coordinate system) at 43/41 Ma ago.

3.4 The Huatung Basin

The Huatung Basin generally deepens northeastward between 3000 and 6000 meters. Hilde and Lee (1984) identified four magnetic polarity reversals (*Anomaly 19* to *Anomaly 16*) in the Huatung Basin. However, the new magnetic anomaly map reveals several new insights into the nature of this basin.

We suggest that the Huatung Basin is composed of three zones separated by two N-S trending old fracture zones (segments H_1H_2 and H_3H_4 in Figure 8). Their existence is confirmed by seismic reflection profiles (e.g., Chen *et al.*, 1996; Liu *et al.*, 1997b; Deschamps, 1997). The area between the EFZ and H_3H_4 consists of faulted oceanic crusts as previously mentioned. Between H_1H_2 and H_3H_4, the Huatung Basin contains six E-W trending magnetic polarity reversals. One positive E-W magnetic lineation seems to be truncated near 122.5° E and 22.7° N, which is more or less along the NE-SW trending Taitung Canyon and should be associated with a major present-day strike-slip fault (Hsu *et al.*, 1996b). However, GPS data (Yu *et al.*, 1997) suggest a NE-SW displacement along the Taitung Canyon only at a rate of 8 mm/yr, if we assume that the relative motion between the Lutao(L) and Lanhsu(Lh) islets is representative (figure 1). This assumption is supported by a number of large earthquakes that have occurred along the Taitung Canyon (Hsu *et al.*, 1996b). The FAA map indicates that the crust northwest of the Taitung Canyon is subsiding with respect to the southeast.

The oceanic basement of the Huatung Basin generally deepens toward the west (Chen *et al.*, 1996). Based on deep seismic reflection profiles, the depth to the oceanic basement of the central portion of the Huatung basin is about 6.2 km (e.g. Chen *et al.*, 1996; Deschamps, 1997). The oceanic basement is overlain by sediments with a thickness of 1.4 km thick. West of H_1H_2, the depth to the oceanic basement increases to about 6.8 km and the sedimentary layer is about 2.4 km thick. The thick sediments in the west are produced by the ample sediment source from eastern Taiwan (Lundberg *et al.*, 1997) and the flexure of the basement due to the load of the Luzon Arc. However, if the depth to the crust increases away from the associated spreading ridge as predicted by the crustal cooling model, then the oceanic crust west of the H_1H_2 is older than that to the east.

It is noted that the character of magnetic anomalies in the northern end of the Huatung Basin changes across a NW-SE trending feature defined by H_5H_6 in Figure 8. To the northeast of this segment, the magnetic reversal pattern is no longer present. Because the direction of segment H_5H_6 is almost parallel to the present convergence direction of the Philippine Sea Plate relative to the Eurasian Plate (Seno *et al.*, 1993), this may suggest that the northern end of the Huatung Basin is a present-day transform margin and is parallel to the general trend of the bent Ryukyu Arc west of 123.5° E (Hsu *et al.*, 1996b).

3.5 The Luzon Arc

In arc-trench systems, most of island arcs are trenchward convex. However, the Luzon Arc is slightly concave toward the Manila Trench as revealed by the FAA map (Figure 5) and

the topography. A major change in segmentation of the Luzon Arc occurs between the Lutao and Lanhsu Islets, where the Taitung Canyon cuts through and trends northeastward (Figure 1; Hsu *et al.*, 1996b). Another apparent internal deformation of the Luzon Arc occurs north of Batan Islet (near 121.9° E and 20.8° N): a possible NE-SW trending strike-slip fault is marked by a bathymetric depression and relatively low FAA. Karig (1973) interpreted a series of discontinuities across the Luzon Arc as left-lateral strike-slip faults; however, existing earthquake focal mechanisms suggest that they could be right-lateral strike-slip faults (e.g. Lewis and Hayes, 1989). The internal deformation of the Luzon Arc is probably responsible for the bending of the arc. North of Batan Islet, the magnetic anomalies associated with the Luzon Arc display a narrow belt with focused "blocks", linked to bathymetric troughs or intra-arc basins (Huang *et al.*, 1995); whereas, the southern portion shows distinctly different characteristics of broader and higher amplitude of magnetic anomalies. This phenomenon may be related to the collision of the Luzon Arc with eastern Taiwan and the "normal" subduction of the South China Sea plate beneath the Luzon Arc.

The northern end of the Luzon Arc can be clearly delineated on the FAA map as far north as 23.7° N. A positive magnetic anomaly however exists north of 23.7° N to 24° N (Figure 8). Its nature is not clear. It might belong to the northernmost Luzon Arc or to the northwesternmost oceanic crust of the Huatung Basin. The low FAA near 121.9° E and 23.8° N could suggest that the Luzon Arc has subsided or partly subducted westward beneath the island of Taiwan. The westward subduction accommodates the extensional tectonics in northern Taiwan and the SE-NW convergence between the Philippine Sea and Eurasian Plates (Hsu and Sibuet, 1995; Angelier *et al.*, 1995; Shemenda *et al.*, 1992). Chemenda *et al.* (1997) suggested a change of subduction polarity from the western side of the Luzon Arc to the eastern side; however, we suggest that the northernmost Luzon Arc has been partly subducted beneath Taiwan.

The Palaui Ridge, located immediately to the east of the Luzon Arc and in the northeastern continuation of Luzon Island (near 122.4° E and 18.7° N), reveals a high FAA (Figures 1 and 5). It has been considered as an inactive subduction complex (Karig, 1973; Lewis and Hayes, 1989); thus, it is noted that the Palaui and Gagua Ridges were not caused by the same mechanism (Lewis and Hayes, 1989), even though they have continuous bathymetry and a continuous low FAA on the east. The low FAA west of the Palaui Ridge displaying a little convex eastward corresponds to the location of an old forearc basin with respect to the former subduction complex (i.e, the Palaui Ridge). Earthquake focal mechanism studies suggest a NE-SW trending right-lateral strike-slip fault along this gravity low (e.g. Lewis and Hayes, 1989).

3.6 The Southwestern Ryukyu Subduction Zone

The south Ryukyu Arc west of 123.5°E exhibits very low magnetic anomalies, indicating low magnetization (Hsu *et al.*, 1997). In contrast, east of 123.5° E the Ryukyu Arc shows dipole fields and NE-SW trends similar to those observed in the middle and northern parts of the Ryukyu Arc. This phenomenon reflects that the magnetic sources rarely exist beneath the upper portion of the Ryukyu Arc west of 123.5° E. The Ryukyu Arc west of 123.5° E could thus be considered as a present-day non-volcanic arc. East of 123.5° E, the Ryukyu Arc exhib-

its diffusive volcanic chains (e.g. Letouzey and Kimura, 1985; Sibuet *et al.*, 1987). If the magnetic isochrons in the Huatung Basin correspond to *Anomaly 19* through *Anomaly 16*, from south to north, as proposed by Hilde and Lee (1984), the corresponding spreading ridge and the counterpart of the Huatung Basin, i.e. the oceanic crust comprising the magnetic isochrons from *Anomaly 13 to Anomaly 19*, must have already subducted beneath the south Ryukyu Arc. This suggests that the Philippine Sea Plate has been subducting beneath the southern Ryukyu Arc since ~7 Ma (assuming the present rate of convergence). However, the depth of the Wadati-Benioff zone, favoring arc volcanism, is located at 100-200 km beneath the central/southern portion of the southern Okinawa Trough (e.g., Kao *et al.*, 1998; Sibuet *et al.*, 1998). This result again agrees with the non-volcanic arc for the south Ryukyu Arc west of 123.5° E.

The forearc basins of the south Ryukyu Arc are marked by rather low oscillating FAA (as low as -230 mGal), corresponding to the Hoping Basin, Nanao Basin and East Nanao Basin from west to east (cf. Figures 1 and 5). These features are also clearly revealed in the Bouguer anomalies (Figure 6). The magnetic anomalies in the backarc region reveal two important characteristics. First, *en echelon* magnetic anomalies trending E-W, associated with recent (probably < 2 Ma old) submarine volcanism could be discerned. This recent backarc volcanism can be attributed to the resumption of the backarc extension after the Luzon Arc swept the Ryukyu Arc west of 123.5° E (Hsu *et al.*, 1996b). Secondly, a magnetic feature trending NW-SE (indicated by O_1O_2 in Figure 8) appears to be associated with Fault A of Hsu *et al.* (1996b). This feature is highly magnetized (Hsu *et al.*, 1997) and is present across the northern margin of the Okinawa Trough, implying that the Okinawa Trough existed prior to the occurrence of Fault A. Another linear magnetic feature (indicated by O_3O_4 in Figure 8) is present along the location of Fault B of Hsu *et al.* (1996b). The presence of Fault B is also marked by an abrupt change in the FAA (Figure 5). The emplacement of volcanic intrusions or extrusions, such as Pengchiayu and Mienhuayu, along the proposed faults (Hsu *et al.*, 1996b; Hsu *et al.*, 1997) is more recent than 2.5 Ma old (Wang *et al.*, 1997). It is noted that the volcanism in the northern margin of the southern Okinawa Trough generally occurs at locations where the depth to the Wadati-Benioff zone is around 200 km (e.g. Kao *et al.*, 1998). This volcanism could be attributed to the post-collisional decoupling of the Okinawa Trough backarc extension from the Luzon Arc collision (Hsu *et al.*, 1996b).

The Ilan Plain and its offshore area are marked by a low FAA trending NE-SW (Figures 1 and 5). Its onshore continuation is along the Lishan Fault (Hsu *et al.*, 1996a). The northern edge of the Ilan Plain is bounded by the NE-SW trending Hsüehshan Range (Figure 1) which may extend offshore according to the FAA map (Figure 5). This NE-SW trending feature inherits the general trend of the Ryukyu arc-trench system, except that the Keelung Submarine Valley (developed along Fault C of Hsu *et al.*, 1996b) cuts through it. The southern edge of the Ilan Plain is bounded by the eastern Central Range of Taiwan and the westernmost segment of the Ryukyu Arc (Figures 1 and 5). The crustal velocity structures of the latter two are similar on the basis of seismic refraction profiles (Cheng *et al.*, 1996) and could belong to the former Ryukyu Arc (Hsu and Sibuet, 1995). The Ilan Plain is also marked by a linear magnetic anomaly, which is convex northward and is continuous from the onshore to the offshore area (Figure 8).

4. CONCLUSION

A new FAA map of the Taiwan-Luzon region has been compiled using the available shipboard, land and satellite-derived data. A simple Bouguer anomaly map is also calculated in order to reduce the effects of topography. A magnetic anomaly map for the same region has also been constructed using shipboard and aeromagnetic data, and a small amount of magnetic data on Taiwan. Due to the uneven distribution of the shipboard data, the compiled data close to Taiwan and the southern part of the Ryukyu Arc is more reliable (see Figures 4 and 7).

The main points from the interpretation of the gravity and magnetic maps in the Taiwan-Luzon region are:

(1) The Peikang High and the Penghu islands in and off southwest Taiwan are located on a major gravity and magnetic belt trending NE-SW. This prominent NE-SW trending belt could be correlated to the Taiwan-Sinzi Folded Belt. The Taishi Basin, marked by a relatively low FAA near 120.3° E and 24.3° N, could correspond to a thickly sedimented, flexural basin.

(2) The NW-SE trending S_1S_2 segment in Figure 8 could delinate a fossil transform fault. Northeast of this boundary, the crust displays low-amplitude gravity and magnetic anomalies and may represent a trapped piece of the Philippine Sea Plate. Southwest of this boundary, the South China Sea exhibits high-amplitude gravity and magnetic anomalies with at least 3 magnetic reversals, which may put back the initial age of the South China Sea opening.

(3) Several E-W trending magnetic reversals are identified in the Huatung Basin and are separated by two old N-S trending fracture zones. The western portion of the basin has the greatest depth to oceanic basement and hence may be the oldest crust in the basin. The central portion contains at least six magnetic reversals. The eastern portion has been influenced by vertical tectonism, producing several N-S trending transverse ridges of the oceanic crust. Among these, the Gagua Ridge is the most prominent.

(4) Compared to the general configuration of island arcs in the world, the Luzon Arc is abnormally concave toward the Manila Trench. The bending of the Luzon Arc could be in response to its collision with eastern Taiwan. Two major changes in segmentation of the Luzon Arc are present: one is between the Lutao and Lanhsu islets and could be linked to a major change in stress condition (Hsu *et al.*, 1996b); the other occurs north of Batan Islet and could be associated with a right-lateral strike-slip fault. South of Batan Islet, the Luzon Arc has a broader distribution of the gravity and magnetic anomalies .

(5) Except for deformation along NW-SE trending strike-slip faults, the structures between the northern Taiwan and south Ryukyu subduction zone are continuous. For example, gravity feature of the Hsüehshan Range in northern Taiwan can be extended northeastward into the sea. Likewise, the eastern Central Range of Taiwan may connect with the south Ryukyu Arc. Magnetic anomaly pattern of the south Ryukyu Arc, west of 123.5° E, is presently a non-volcanic arc. The post-collisional volcanism has occurred along the existing NW-SE trending faults at the northern margin of the southern Okinawa Trough.

Acknowledgments We are indebted to Dr. Horng-Yuan Yen for the gravity ties at Keelung and Kaoshiung harbors. Dr. Cheng-Horng Lin provided geomagnetic data from the Hualien

observatory. Constructive reviews from Drs. C.-S. Lee and T.-Y. Lee are appreciated. This study was supported by the National Science Council, Taiwan, Republic of China under grants NSC86-2811-M002-0001 and NSC87-2811-M002-002.

REFERENCES

Abrams, L. J., R. S. Detrick, and P. J. Fox, 1988:Morphology and crustal structure of the Kane fracture zone transverse ridge. *J. Geophys. Res.*, 93, 3195-3210.

Angelier, J., J. C. Lee, H. T. Chu, C. Y. Lu, M. Fournier, J. C. Hu, N. T. Lin, B. Deffontaines, B. Delcaillau, O. Lacombe, and T. Q. Lee, 1995: Crustal extension in an active orogen: Taiwan, ACT International Conference and 3rd Sino-French Symposium on Active Collision in Taiwan, Program and extended abstracts, 22nd-23rd March, Geol. Soc. China, Taiwan, R.O.C., 25-32.

Bonatti, E., 1978: Vertical tectonism in oceanic fracture zones. *Earth Planet. Sci . Lett.*, **37**, 369-379.

Bosum, W., G. D. Burton, S. H. Hsieh , E. G. Kind, A. Schreiber, and C. H. Tang, 1970: Aeromagnetic survey of offshore Taiwan. *CCOP Technical Bulletin, ECAFE*, **3**, 1-34.

Bowin C., R. S. Lu, C. S. Lee, and H. Schouten, 1978: Plate convergence and accretion in Taiwan-Luzon region. *AAPG Bulletin*, 62, 1645-1672.

Briais, A., P. Patriat, and P. Tapponnier, 1993: Updated interpretation of magnetic anomalies and seafloor spreading stages in the South China Sea: Implications for the Tertiary tectonics of southeast Asia. *J. Geophys. Res.*, **98**, 6299-6328.

Cande S. C, and D.V. Kent, 1995: Revised calibration of the geomagnetic polarity timescale for the Late Cretaceous and Cenozoic. *J. Geophys. Res.*, **100**, 6093-6095.

Chang, S. S. L., and C. C. Hu, 1981: Gravity and magnetic anomalies of Taiwan and their tectonic implication. *Mem. Geol. Soc. China*, **4**, 121-142.

Chen, P. J., R. C. Shih, Y. H. Yeh., C. S. Liu, C. H. Lin, C. H., H. Y. Yen, B. S. Huang, 1996: Analysis and interpretation of the Taiwan sea-land joint seismic profile (southern cross-island highway), Proceedings of the sixth Taiwan Symposium on Geophysics, 727-736.

Cheng, W. B., C. Wang, and C. T. Shyu, 1996: Crustal structure of the northeastern Taiwan area from seismic refraction data and its tectonic implications. *TAO*, **7**, 467-487.

Chi, W. R., 1996: Basin characterization, tectonic evolution, and hydrocarbon potential of the offshore and onshore Taiwan sedimentary basins, CPC exploration and research reports, 82-114. (in Chinese with English abstract)

Deschamps, A., 1997: Signification tÈctonique de la ride de Gagua en subduction prËs de Taiwan, DEA thesis, Univ. Sci. Tech. Languedoc, AcadÈmie de Montpellier, 41pp.

Deschamps, A., S. Lallemand, and J. Y. Collot, 1997: The tectonic significance of the Gagua ridge near Taiwan, International conference and Sino-American symposium on tectonics of East Asia, Programme and Abstracts, 3-5 November 1997, 142.

Hilde, T. W. C., and C. S. Lee, 1984: Origin and evolution of the West Philippine Basin: a new interpretation. *Tectonophysics*, **102**, 85-104.

Hsu, S. K, 1995: A cross-over technique to adjust track data. *Compu. & Geosci.*, **21**, 259-271.

Hsu, S. K., and J. C. Sibuet, 1995: Is Taiwan the result of arc-continent or arc-arc collision?. *Earth Planet. Sci . Lett.*, **136**, 315-324.

Hsu, S. K., J. C. Sibuet, and C. T. Shyu, 1996a: High-resolution detection of geologic boundaries from potential-field anomalies: an enhanced analytic signal technique. *Geophysics*, **61**, 373-386.

Hsu, S. K., J. C. Sibuet, S. Monti, C. T. Shyu, and C. S. Liu, 1996b: Transition between the Okinawa trough backarc extension and the Taiwan collision: new insights on the southernmost Ryukyu subduction zone. *Mar. Geophys. Res.*, **18**, 163-187.

Hsu, S. K., C. T. Shyu, C. S. Liu, L. Y. Chiao, J. C. Sibuet, and S. Y. Liu, 1997: Tectonic features of the southern Okinawa trough: results from marine geophysical data analysis, Proceedings of the Chinese Geophysical Meeting, 277-281.

Hu, C. C., and R. S. Lu, 1979: Downward continuation of magnetic field and magnetic anomalies of offshore Taiwan. *Acta Oceanographica Taiwanica.*, **9**, 1-8.

Hu, C. C., and W. S. Chen, 1986: Gravity and magnetic anomalies of eastern Taiwan. *Mem. Geol. Soc. China*, **7**, 341-352.

Hwang, C. W., and B. Parsons, 1996: An optimal procedure for deriving marine gravity from multi-satellite altimetry. *Geophys. J. Int.*, **125**, 705-718.

Hwang, W. T., and C. Y. Wang, 1993: Sequential thrusting model for mountain building: constraints from geology and heat flow of Taiwan. *J. Geophys. Res.*, **98**, 9963-9973.

Huang, C. Y., P. B. Yuan, S. R. Song, C. W. Lin, C. Wang, M. T. Chen, C. T. Shyu, and B. Karp, 1995: Tectonics of short-lived intra-arc basins in the arc-continent collision terrane of the Coastal Range, eastern Taiwan. *Tectonics*, **14**, 19-38.

IAGA (International Association of Geomagnetism and Aeronomy) Division V, Working Group 8, 1996: International geomagnetic reference field, 1995 revision. *Geophys. J. Int.*, **125**, 318-321.

Kao, H., S. J. Shen, and K. F. Ma, 1998: Transition from oblique subduction to collision: earthquakes in the southernmost Ryukyu arc-Taiwan region. *J. Geophys. Res.*, **103**, 7211-7229.

Karig, D. E., 1973: Plate convergence between the Philippines and the Ryukyu islands. *Mar. Geol.*, **14**, 153-168.

Karp, B. Y., R. Kulinich, C. T. Shyu, and C. Wang, 1997: Some features of the arc-continent collision zone in the Ryukyu subduction system, Taiwan Junction area. *The Island Arc*, **6**, 303-315.

Lallemand, S. E., C. S. Liu, and the ACT cruise scientific team, 1997: Swath bathymetry reveals active arc-continent collision near Taiwan. *EOS, Trans. AGU*, **78**, 173-175.

Lee, C. R., and W. T. Cheng, 1986: Preliminary heat flow measurements in Taiwan, paper presented at fourth Circum-Pacific Energy and Mineral Resources Conference, Singapore.

Lee, C. S., and R. S. Lu, 1976: Significance of the southwestern section of Ryukyu inner ridge

in the exploration of geothermal resources in Ilan area. *Mining Technical Digest*, **14**, 114-120. (in Chinese)

Lee, C. S., and T. W. C. Hilde, 1971: Magnetic lineations in the western Philippine Sea. *Acta Oceanographica Taiwanica*, **1**, 69-75.

Lee, T. Y., 1993: Sequence stratigraphy of the Tainan Basin, offshore southwestern Taiwan. *Petrol. Geol. Taiwan*, **28**, 119-158.

Letouzey, J., and M. Kimura, 1985: Okinawa trough genesis: structure and evolution of a backarc basin developed in a continent. *Marine and Petroleum Geology*, **2**, 111-130.

Lewis, S. D., and D. E. Hayes, 1989: Plate convergence and deformation, North Luzon Ridge, Philippines. *Tectonophysics*, **168**, 221-237.

Liu, C. S., S. Y. Liu, S. E. Lallemand, N. Lundberg, and D. Reed, 1998: Digital elevation model offshore Taiwan and its tectonic implications. *TAO, 9,* (accepted).

Liu, C. S., I. L. Huang, and L. S. Teng, 1997a: Structural features off southwestern Taiwan. *Mar. Geol.*, **137**, 305-319.

Liu, C. S., S. Y. Liu, B. Y. Kuo, N. Lundberg, D. L. Reed, 1992: Characteristics of the gravity and magnetic anomalies off southern Taiwan. *Acta Geologica Taiwanica*, **33**, 121-130.

Liu, C. S., P. Schnurle, S. Lallemand, and D. L. Reed, 1997b: Crustal structures of the Philippine Sea plate near Taiwan, International conference and Sino-American symposium on tectonics of East Asia, Programme and Abstracts, 3-5 November 1997, 54-55.

Liu, S. Y., 1993: The bathymetric, gravimetric and magnetic characteristics of Taiwan - North Luzon area: tectonic evolution from normal subduction to arc-continent collision, Master's thesis, National Taiwan University, 79pp. (in Chinese)

Lundberg, N., D. L. Reed, C. S. Liu, and J. Lieske, Jr., 1997: Forearc-basin closure and arc accretion in the submarine suture zone south of Taiwan. Tectonophysics, **274**, 5-23.

Magnetic Anomaly Map of East Asia, 1994: *In* Geological Survey of Japan and Committee for coordination of joint prospecting for mineral resources in Asian offshore areas (CCOP).

McCarthy, M. C., S. E. Kruse, M. R. Brudzinski, and M. E. Ranieri, 1996: Changes in plate motions and the shape of Pacific fracture zones.. *J. Geophys. Res.*, **101**, 13715-13730.

Mrozowski, C. L., S. D. Lewis, and D. E. Hayes, 1982: Complexities in the tectonic evolution of the West Philippine Basin. *Tectonophysics*, **82**, 1-24.

Oshida, A., K. Tamaki, and M. Kimura, 1992: Origin of the Magnetic anomalies in the southern Okinawa trough. *J. Geomag. Geoelectr.*, **44**, 345-359.

Reed, D., N. Lundberg, C. S. Liu, and B. Y. Kuo, 1992: Structural relations along the margins of the offshore Taiwan accretionary wedge: implication for accretion and crustal kinematics. *Acta Geologica Taiwanica*, **30**, 105-122.

Regan, R., and P. Rodriguez, 1981: An overview of the external magnetic field with regard to magnetic surveys. *Geophys. Surv.*, **4**, 255-296.

Sandwell, D. T., 1984: Thermomechanical evolution of oceanic fracture zones. *J. Geophys. Res.*, **89**, 11401-11413.

Sandwell, D. T., and W. H. F. Smith, 1997: Marine gravity anomaly from Geosat and ERS 1 satellite altimetry. *J. Geophys. Res.*, **102**, 10039-10054.

Schnürle, P., C. S. Liu, D. Reed, D., and S. E. Lallemand, 1998: Structural Controls of the Taitung Canyon in the Huatung Basin East of Taiwan. *TAO*, **9**, 453-472.

Seno, T., S. Stein, and A. E. Gripp, 1993: A model for the motion of the Philippine Sea Plate with NUVEL-1 and geological data. *J. Geophys. Res.*, **98**, 17941-17948.

Shemenda, A. I., C. H. Hsieh, and R. K. Yang, 1992: Reversal subduction and a geodynamic model of the collision in Taiwan. *Acta Geologica Taiwanica*, **30**, 101-104.

Shyu, C. T., and L. Y. Chiao, 1983: Trends of the magnetic anomalies in the immediate offshore area of the Ilan plain, Taiwan. *Acta Oceanographica Taiwanica*, **14**, 16-25.

Shyu, C. T., and S. C. Chen, 1991: A topographic and magnetic analysis off southeastern Taiwan. *Acta Oceanographica Taiwanica*, **27**, 1-20.

Shyu, C. T., M. C. Chih, S. K. Hsu, C. Wang, and B. Karp, 1996: Northern Luzon arc: location and tectonic features from magnetic data off eastern Taiwan. *TAO*, **7**, 535-548.

Sibuet, J. C., and S. K. Hsu, 1997: Geodynamics of the Taiwan arc-arc collision. *Tectonophysics*, **274**, 221-251.

Sibuet, J. C., B. Deffontaines, S. K. Hsu, N. Thareau, J. P. Le Formal, C. S. Liu, and the ACT party, 1998: Okinawa trough backarc basin: early tectonic and magmatic evolution. *J. Geophys. Res.*, (in press)

Sibuet, J. C., J. Letouzey, F. Barrier, J. Charvet, J. P. Foucher, T. W. C. Hilde, M. Kimura, L. Y. Chiao, B. Marsset, C. Muller, C., and J. F. StÈphan, J. F., 1987: Back arc extension in the Okinawa trough. *J. Geophys. Res.*, **92**, 14041-14063.

Small, C., and D. T. Sandwell, 1992: A comparison of satellite and shipboard gravity measurements in the Gulf of Mexico. *Geophysics*, **57**, 885-893.

Swan, D., and I. F. Young, 1978: Crossover differences as an indication of survey accuracy. *Mar. Geophys. Res.*, **3**, 393-400.

Taylor, B., and D. E. Hayes, 1983: Origin and history of South China Sea Basin. In: D.E. Hayes (Ed.), The Tectonic and Geologic Evolution of Southeast Asian Sea and Islands, 2, AGU, Washington, DC., 23-56.

Wang, C., and T. W. C. Hilde, 1973: Geomagnetic interpretation of the geologic structure in the northeast offshore region of Taiwan. *Acta Oceanographica Taiwanica*, **3**, 141-156.

Wang, K. L., S. L. Chung, C. H. Chen, T. F. Yang, and C. H. Chen, 1997: New observations on geochemical characteristics of volcanic rocks from the northern Taiwan volcanic zone (NTVZ), 1997 Annual Meeting of Geological Society of China, Program and Expanded Abstracts, 407-411.

Wessel, P., and W. H. F. Smith, 1991: Free software helps map and display data. *EOS trans. Amer. Geophys. U.*, **72**, 441, 445-456.

Wu, Y. M, 1991: Geophysical studies on the boundary between the eastern Taiwan (Latitude 23-Latitude 24) and the Philippine Sea plate, Master's thesis, National Taiwan Ocean University, 78pp. (in Chinese)

Yang, C. H., T. C. Shei, and C. C Lue, 1994: Gravity and magnetic studies in the Tatun volcanic region. *TAO*, **5**, 499-514.

Yeh, Y. H., E. Barrier, C. H. Lin, and J. Angelier, 1991: Stress tensor analysis in the Taiwan area from focal mechanism of earthquakes. *Tectonophysics*, **200**, 267-280.

Yen, H. Y., W. T. Liang, B. Y. Kuo, Y. H. Yeh, C. S. Liu, D. Reed, N. Lundberg, F. C. Su, and H. S. Chung, 1995: A regional gravity map for the subduction-collision zone near Taiwan. *TAO*, **6**, 233-250.

Yen, H. Y., Y. H. Yeh, C. H. Lin, G. K. Yu, and Y. B. Tsai, 1990: Free-air gravity map of Taiwan and its application. *TAO*, **1**, 143-156.

Yu, H. S., 1994: Structure, stratigraphy and basin subsidence of Tertiary basins along the Chinese southern continental margin. *Tectonophysics*, **235**, 63-76.

Yu, H. S., and C. T.Shyu, 1994: Topography, geomagnetism and structure in the shelf-slope region off northeastern Taiwan. *J. Geol. Soc. China*, **37**, 247-260.

Yu, H. S., and C. T. Lee, 1993: The multi-head Penghu submarine canyon off southwestern Taiwan: morphology and origin. *Acta Oceanographica Taiwanica*, **30**,10-21.

Yu, H. S., and J. C. Lu, 1995: Development of the shale diapir-controlled Fangliao Canyon on the continental slope off southwestern Taiwan. *J. South. Asian Earth Sci.*, **11**, 265-276.

Yu, S. B, and Y. B. Tsai, 1979: Geomagnetic anomalies of Ilan plain, Taiwan. *Petr. Geol. Taiwan.*, **16**, 19-27.

Yu, S. B, and Y. B. Tsai, 1981: Geomagnetic investigation in the Pingtung plain, Taiwan. *Bull. Inst. Earth Sci. Academia Sinica*, **1**, 189-208.

Yu, S. B., H. Y. Chen, and L. C. Kuo, 1997: Velocity field of GPS stations in the Taiwan area. *Tectonophysics*, **274**, 41-59.